Thioether-based poly(2-oxazoline)s: from optimized synthesis to advanced ROS-responsive nanomaterials†

Semira Bener, [ID] [a] Ewa Pavlova, [ID] [b] Hynek Beneš [ID] [b] and Ondřej Sedláček [ID] *[a]

Intelligent redox-responsive polymers, such as thioether-containing macromolecules, facilitate drug delivery and triggered release in biomedical applications. Moreover, reactive oxygen species (ROS)-responsive thioether systems based on poly(2-oxazoline)s (PAOx) platforms hold great promise for the development of highly biocompatible, stimuli-responsive biomaterials. However, thioether-containing PAOx are particularly difficult to synthesize because thioethers are incompatible with the cationic ring-opening polymerization (CROP). In this study, we aim at developing an alternative route to well-defined thioether-containing PAOx by a simple post-polymerization modification of linear polyethyleneimine. First, the synthesis of ROS-responsive PAOx homopolymers was optimized. Furthermore, ROS-sensitive amphiphilic diblock copolymers poly(ethylene glycol)-*block*-poly(2-methylthiomethyl-2-oxazoline) were synthesized by combining CROP with 2-oxazoline side-chain interchange *via* a polyethyleneimine block intermediate. In an aqueous environment, the copolymers self-assembled into thioether-containing micelles. These micelles were characterized by size exclusion chromatography, nuclear magnetic resonance, matrix-assisted laser desorption/ionization-time of flight mass spectrometry, dynamic light scattering, differential scanning calorimetry, and transmission electron microscopy. In addition, treatment with diluted H_2O_2 destabilized the nanoparticles, thus demonstrating their oxidation-responsiveness. This approach provides key insights into the design and development of stimuli-responsive polymers for potential biomedical applications, such as drug delivery systems.

[a]Department of Physical and Macromolecular Chemistry, Faculty of Science, Charles University, Prague 2 128 40, Czech Republic. E-mail: sedlacek@natur.cuni.cz
[b]Institute of Macromolecular Chemistry, AS CR, Prague 6 162 06, Czech Republic
†Electronic supplementary information (ESI) available. See DOI: https://doi.org/10.1039/d3py00945a

Introduction

Over the past century, several studies have analyzed supramolecular nanostructures generated by the self-assembly of amphiphilic block copolymers for their stability as drug carriers.[1–4] Such nanostructures have been extensively used in bio-inspired applications, including drug delivery and nanoreactors, thanks to their broad range of topologies, including micelles, vesicles, and nanogels.[5] Among these applications, self-assembled nanoparticles composed of biocompatible and biodegradable polymers have been explored for anticancer drug encapsulation for their high potential to improve the solubility of a drug in water, prolonging its blood half-life while simultaneously reducing its systemic toxicity.[6–8]

Another key feature of these systems is their ability to trigger the controlled release of their encapsulated content.

This feature has prompted extensive research on the engineering mechanisms of drug carriers and generated major advances in the design of such systems responsive to various stimuli. By harnessing intrinsic triggers, these advancements have improved excretion from the body and enhanced the therapeutic potential of targeted applications through a more effective and controlled drug release in response to pH,[9] temperature,[10,11] redox,[12] ultrasound[13] and light[14,15] stimuli.

Reactive oxygen species (ROS), particularly hydrogen peroxide (H_2O_2), hydroxyl radicals (•OH), the superoxide anion radical ($O_2^{•-}$), and nitrites ($ONOO^-$), play a key role in regulating fundamental physiological processes in living organisms, including cellular growth, cell signaling, modulation of protein function, and stress adaptation.[16,17] While ROS are maintained at basal levels in healthy cells, elevated levels are often found in pathogenic cells, as a result of high metabolic activity or inflammation due to conditions such as cancer or neurodegenerative diseases. Many delivery systems have been recently developed to release therapeutic cargos in response to ROS for target–specific drug delivery. The oxidative response of these systems is consistently based on the oxidation of the hydrophobic moieties leading to strongly hydrophilic poly-

meric materials that disassemble upon oxidation, thereby releasing the incorporated cargo.[18] Invariably, these hydrophilic polymers contain oxidation–sensitive moieties, such as sulfides, diselenides, thioketals, aryl boronic esters, and thioethers.[19,20]

Thioether-containing polymer systems have demonstrated potential in ROS-responsive applications due to the unique reactivity of sulfur to ROS.[21] Polymers incorporating thioether groups can be designed to be responsive to ROS, such as glutathione, by undergoing a hydrophobic-hydrophilic phase transition from thioethers with low dipole moments to a hydrophilic sulfoxide or sulfone in response to ROS, leading to an efficient disassembly of the materials.[22] Thus, their disassembly enables the targeted and controlled release of drugs or other cargos based on the hydrophobic-hydrophilic phase transition of their thioether groups.

Poly(2-oxazoline)s (PAOx) represent an emerging class of polymers for the construction of amphiphilic block copolymer nanoparticles that can be precisely controlled and adjusted for specific applications thanks to their versatility and relatively straightforward synthesis.[23–27] The properties of PAOx can be fine-tuned by varying the monomer as the side-chain substituent of 2-oxazoline can be replaced widely and readily.[28] Furthermore, living cationic ring-opening polymerization (CROP) provides control over the resulting copolymeric structure and access to end-functionalized polymer chains with a wide range of functional groups.[29,30] Thioether-containing poly(2-oxazoline)s offer several advantages over analogous thioether-containing polymers derived from, e.g., polyacrylamides,[31] even though their synthesis can be somewhat more complex. The increased flexibility of the poly(2-oxazoline) backbone,[32] in contrast to acrylic polymers, could potentially enhance nanoparticle self-assembly and enable the encapsulation of drugs.[33] Additionally, these more flexible polymers exhibit accelerated diffusion into cancerous tissues, leading to greater accumulation within tumors. Yet, despite their potential benefits, thioether-containing PAOx polymers are still difficult to synthesize. Polymers containing specific side chain groups, such as free amines, alcohols, thiols, and carboxylic acids cannot be prepared by CROP because of potential terminations, chain transfer, and side reactions via a nucleophilic attack on the propagating cationic oxazolinium species.[34–36] In this context, 2-((methylthio)methyl)-2-oxazoline has been polymerized using methyl tosylate and methyl triflate as a more electrophilic initiator.[37–39] However, this polymerization was not controlled, showing a steep initial increase in molar masses at a low monomer conversion rate, which indicates the occurrence of side reactions during the polymerization, most likely caused by the thioether bond. Moreover, the nucleophilic thioether group could induce termination and transfer reactions by attacking the oxazolinium group and forming a sulfonium ion. Nevertheless, functional groups can be incorporated into the PAOx polymeric chain by post-polymerization modifications.[40–42]

Post-polymerization acylation of PEI is a straightforward method for preparing well-defined, functional PAOx, as described recently.[32,35,43–45] By using this approach, we can synthesize diverse poly(2-oxazoline) (PAOx) libraries using various carboxylic acids. This method also eliminates the need for functional monomer synthesis and purification, which are often challenging and time-consuming processes, and extends to the synthesis of random PAOx copolymers, especially when monomers with different reactivities yield gradient copolymer structures, such as MeOx with PhOx. Concomitantly, the reacetylation of linear polyethyleneimine (PEI) prepared via hydrolysis of poly(2-methyl-2-oxazoline) (PMeOx) with acetic anhydride for PAOx synthesis is a promising alternative to conventional CROP, particularly for monomers with functionalities that can act as terminators of CROP.[46–50] Therefore, we aimed at developing an alternative route to thioether-containing PAOx by a simple post-polymerization modification of linear PEI prepared via hydrolysis of readily available PEtOx.

In this study, we report the synthesis of novel oxidation-sensitive PAOx by post-polymerization side chain interchange via a linear PEI intermediate. First, we prepared a series of three leading thioether-containing PAOx homopolymers using three different alkylthiocarboxylic acids. The polymers were well-defined and showed oxidation responsivity. In addition, we synthesized poly(ethylene glycol)-block-poly(2-methyl-thiomethyl-2-oxazoline) (PEG-b-PMTMeOx) amphiphilic diblock copolymers by combining CROP with the reacylation method. Once PEG-b-PEtOx was synthesized by CROP, the copolymer side chain groups were selectively removed by acidic hydrolysis, resulting in a linear PEG-b-PEI, which was further reacylated with a thioether-containing carboxylic acid. Aqueous self-assembly of the PEG-b-PMTMeOx diblock copolymers with different PAOx lengths was examined using the solvent switch method. The micelles containing thioether groups were treated with H_2O_2 to demonstrate the destabilization of the micellar structure. Self-assembly was then investigated by dynamic light scattering (DLS) and transmission electron microscopy (TEM).

Experimental section

Materials

Poly(ethylene glycol) monomethyl ether (PEG, 2000 g mol^{-1}), triethylamine (TEA), p-nitrobenzenesulfonyl chloride, (benzotriazole-1-yloxy) tripyrrolidinophosphonium hexafluorophosphate (PyBOP), (methylthio)acetic acid, (methylthio)propionic, and (ethylthio)acetic acid were purchased from Sigma-Aldrich and used as received. 2-Ethyl-2-oxazoline (EtOx) was purchased from Sigma-Aldrich and distilled over CaH$_2$. Linear polyethyleneimine (PEI, DP = 100) was synthesized from PEtOx, according to the literature.[43]

Synthesis of thioether-containing PAOx homopolymers. To synthesize the homopolymers, a solution of PyBOP (6.98 mmol, 1.5 eq.) and the respective thioether-containing carboxylic acid (methylthioacetic acid, methylthiopropanoic acid and, ethylthioacetic acid, respectively, 6.98 mmol, 1.5 eq.) were dissolved in dry N,N-dimethylacetamide (DMAc, 30 mL).

TEA (13.95 mmol, 3 eq.) was then added dropwise, the resulting mixture was stirred at room temperature, and a solution of linear PEI (200 mg, 1 eq.) in dry DMF (30 mL) was added, continuously stirring overnight (14 h) under an argon atmosphere. Subsequently, the solvent was removed under reduced pressure, and the polymer was isolated through dialysis (MWCO = 1 kDa) against an acetonitrile–water mixture and then distilled water, followed by freeze-drying. The complete conversion of secondary amines was confirmed by ^{1}H NMR spectroscopy.

Synthesis of PEG-ONs macroinitiator. PEG (2000 g mol^{-1}) (4 g, 2 mmol, 1 eq.) was dissolved in 100 mL of dry dichloromethane (DCM) and stirred at 0 °C. Triethylamine (2.8 mL, 20 mmol, 10 eq.) and *p*-nitrobenzenesulfonyl chloride (4.4362 g, 20 mmol, 10 eq.) were added to the solution, which was stirred at 0 °C overnight under an inert atmosphere. The reaction mixture was then concentrated under a vacuum, and the high excess of unreacted reagents was extracted 3 times with 500 mL of isopropanol at room temperature. The polymer was then recrystallized 3 times from EtOH, and the precipitate was filtered and stored under an inert atmosphere. The chain-end modification was confirmed by ^{1}H NMR and MALDI-TOF.

Synthesis of PEG-*b*-PEtOx diblock copolymers. Three block copolymers PEG-*b*-PEtOx, were synthesized by EtOx CROP using PEG-ONs as macroinitiators at different initial monomer/macroinitiator molar ratios (and thus different degrees of polymerizations of the PEtOx block), namely 30, 60, and 100, respectively, with an initial EtOx concentration of 3 M. The polymerization reaction was performed in a microwave reactor (Biotage) in dry acetonitrile at 130 °C under an argon atmosphere for 12 (DP 30), 24 (DP 60), and 40 (DP 100) minutes, respectively. The polymerization mixture was cooled to room temperature, terminated with several drops of water, and precipitated in diethyl ether, followed by filtration and drying under vacuum. The copolymers were obtained as white powders.

Side-chain hydrolysis of PEG-*b*-PEtOx. PEG-*b*-PEtOx diblock copolymers (0.4 g) were dissolved in aqueous hydrochloric acid (19 wt%, 80 mL) and heated at 100 °C for 5 h under an inert atmosphere. All volatiles were removed under vacuum, and the crude polymer was treated with dilute sodium carbonate. The polymers were isolated and purified by dialysis (MWCO = 1 kDa) against distilled water and freeze-dried, yielding PEG-*b*-PEI copolymers.

Synthesis of thioether-containing PEG-*b*-PMTMeOx. The general acylation procedure involved dissolving PyBop (1.5 eq.) and methylthioacetic acid (1.5 equivalents) in dry DMAc (30 mL). Triethylamine (39.3 mL, 3 equivalents) was then added dropwise to the solution, which was stirred at room temperature. Subsequently, the mixture was transferred to a solution of PEG-*b*-PEI (200 mg, 1 equivalent) in dry DMF and stirred overnight under an inert atmosphere. The solvent was then removed under reduced pressure, and the resulting polymers were isolated through dialysis against an acetonitrile–water mixture and then distilled water, followed by freeze-drying.

Polymer characterization

Size Exclusion Chromatography (SEC) was used to determine the molar masses (M_w, mass-averaged molecular weight; M_n, number-averaged molecular weight) and dispersity ($Đ = M_w/M_n$) of the polyoxazoline polymers on a Watrex Streamline system equipped with a Streamline P1 Pump, a Streamline AS2 Autosampler, a Streamline CT Column Thermostat, a Streamline UV detector, and a Streamline RI detector. The separation was performed on two PLgel 5 μm mixed-D columns in a series thermostatted at 55 °C in *N,N*-dimethylacetamide (DMAc) containing 50 mM of LiCl at an elution rate of 0.5 mL min^{-1}. Molar masses and dispersities were calculated against narrow dispersity poly(methyl methacrylate) standards. Linear PEI was measured using Ultimate 3000 system (Dionex) equipped with a TSKgel G5000PWXL-CP 300 × 7.8 mm SEC column. Three detectors, UV/vis, refractive index (RI) Optilab-rEX and multiangle light scattering (MALS) DAWN EOS (Wyatt Technology) were employed; with a methanol and sodium acetate buffer (0.3 M, pH 6.5) mixture (80 : 20 vol%, flow rate of 0.5 mL min^{-1}) as mobile phase using dn/dc = 0.169.

Nuclear Magnetic Resonance (NMR) spectra were recorded on a Bruker Avance MSL 400 MHz NMR spectrometer at 25 °C in CD$_3$OD or DMSO-d$_6$. All chemical shifts are given in ppm.

Matrix-assisted laser desorption/ionization-time of flight mass spectrometry (MALDI-TOF MS) was performed on a Microflex LT MALDI-TOF MS (Bruker Daltonics) mass spectrometer. All mass spectra were recorded at an accelerating potential of 20 kV in positive ion mode and in reflectron mode (matrix:2-[3-(4-tert-butylphenyl)-2-methyl-2-propenylidene] malononitrile (DCTB)). The samples were applied to the MALDI plate using the dried drop method. All measurements were calibrated using poly(ethylene glycol) monomethyl ether (PEG, M_n = 2000 Da).

Dynamic light scattering (DLS) measurements were used to determine the hydrodynamic diameters of the polymers in distilled water on a ZEN3600 Zetasizer Nano-ZS zeta potential analyzer (Malvern Instruments, UK). The apparent *Z*-averaged hydrodynamic diameter of the particles, D_h, was determined at a scattering angle of $\theta = 173°$, and the DTS (Nano) program was used to evaluate the data.

Differential Scanning Calorimetry (DSC) was performed on a DSC Q2000 (TA Instruments, USA) with a nitrogen purge gas (50 mL min^{-1}). Indium was used as a standard for temperature and enthalpy calibrations. Samples of about 5 mg were encapsulated into aluminum pans. DSC runs were performed with a ramp rate of 10 °C min^{-1} using a heating–cooling–heating cycle from −80 °C to 150 °C. The glass transition temperature (T_g) and ΔC_p values were determined from the second heating run.

Transmission Electron Microscopy (TEM) observations were conducted under a Tecnai G2 Spirit Twin microscope operating at an accelerating voltage of 120 kV in bright-field imaging mode. Polymer nanoparticles (4 μL) were applied onto a copper TEM grid (300 mesh) coated with a thin, electron-transparent carbon film. To prevent oversaturation during the

drying process, excess solution was removed by gently touching the bottom of the grid with filtering paper after 5 minutes of sedimentation. Subsequently, the samples were negatively stained with uranyl acetate (2 µL of 1 wt% solution applied onto the dried nanoparticles and removed after 30 seconds) and left to dry at room temperature before their observation under the TEM microscope.

Results and discussion

The synthetic approach to the preparation of thioether-containing PAOx homopolymers is illustrated in Scheme 1. This approach involved a controlled reacylation of linear polyethyleneimine (PEI). PEI was obtained from PEtOx by controlled acidic hydrolysis of its side-chain groups.[51]

The starting material, a well-defined poly(2-ethyl-2-oxazoline) (PEtOx) with a degree of polymerization (DP) of 100, was synthesized by living CROP of EtOx in acetonitrile. This polymerization was terminated with sodium azide to introduce the semitelechelic azide group for potential conjugations. Furthermore, the azide group is inert to the acylation procedure,[43] unlike the frequently used hydroxy or amine groups, which can be acylated by carboxylic acids to their esters or amides. The resulting PEtOx was treated with concentrated hydrochloric acid to yield linear PEI, which was reacylated with a series of thioether-containing carboxylic acids (Table 1) to prepare a library of new PAOx.

Controlled acylation of linear PEI enables us to synthesize PAOx containing highly functional side-chain groups otherwise unattainable by CROP of the respective monomers, as previously reported.[43] PEI amidation was achieved by peptide coupling using (benzotriazole-1-yloxy)-tripyrrolidinophosphonium hexafluorophosphate (PyBOP) as the coupling agent, triethylamine (TEA) as the base and DMAc as the solvent, thereby yielding the new thioether-containing PAOx homopolymers. In this study, polyethyleneimine (PEI) was reacylated with three different thioether-containing carboxylic acids (Table 1) to prepare a library of poly(2-alkylthioalkyl-2-oxazoline) (PAOx) homopolymers. The resulting thioether PAOx homopolymers were comprehensively analyzed using various techniques, including ^{1}H NMR spectroscopy (Fig. 1 and S1†) and SEC (Fig. 2).

The structures of the homopolymers were confirmed by ^{1}H NMR, lacking the signal at 2.8 ppm corresponding to the PEI methylene units. To rule out a potential overlap of the PEI methylene signal with the PAOx side-chain signal (PMTMeOx, PMTEtOx), the peaks were further deconvoluted by 2D ^{1}H/^{13}C HSQC NMR spectroscopy (Fig. S2†). Furthermore, the presence of remaining secondary amines was excluded by a negative Kaiser test with ninhydrin.[43] New peaks corresponding to the PAOx side chains and the typical PAOx backbone peak at 3.4 ppm appeared in the spectra. In addition, the signals of PMTMeOx and PMTEtOx were assigned by ^{1}H/^{1}H COSY NMR.

Since many biological properties of polymers, such as renal clearance, biodistribution, and cellular uptake, are affected by their size, achieving a high level of uniformity in polymer size is generally desirable. All polymers prepared in this study had distinct structures, with narrow molar mass distributions ($Đ \sim$ 1.2). Nevertheless, the SEC chromatograms displayed minor high molar mass shoulder formations, which can be attributed to chain coupling side reactions during the acylation procedure (Fig. 2). As this high molar mass shoulder is most distinct in the chromatogram of PMTEtOx, it might arise from the base-catalyzed elimination of methanethiol followed by intramolecular chain coupling through the side chains.

The thermal characteristics of the newly synthesized thioether poly(2-oxazoline) (PAOx) homopolymers were also investigated by differential scanning calorimetry (DSC). DSC analysis revealed that all the polymers were amorphous, as indicated by the absence of melting transitions, with glass transition temperatures (T_g) ranging from 12 to 48 °C (Table 1 and Fig. 3). Amorphous polymers with low T_g have several advantageous characteristics, such as high chain flexibility and mobility. High chain flexibility accelerates dissolution. In turn, (i) the high chain mobility of low-T_g polymers facilitates both the formation of various self-assembling architectures by
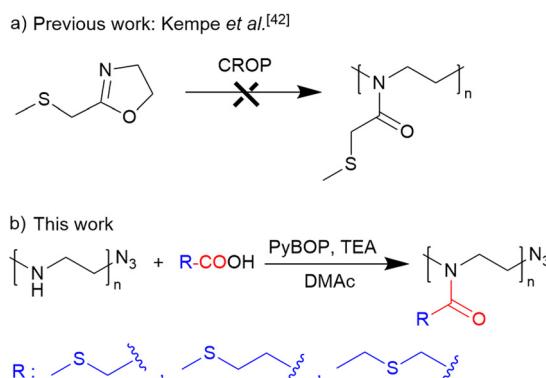
Scheme 1 (a) Schematic representation of the unsuccessful CROP of 2-methylthiomethyl-2-oxazoline[42] and (b) synthesis of thioether-containing homopolymers via acylation of well-defined PEI.

Table 1 Characteristics of thioether-containing PAOx synthesized in this study

Polymer	R-COOH[a]	M_w[b] (kDa)	M_n[b] (kDa)	$Đ$[b]	T_g[c] (°C)	ΔC_p (J g^{-1} °C^{-1})
PMTMeOx	2-(Methylthio)acetic acid	15.9	14.1	1.1	48.0	0.46
PMTEtOx	3-(Methylthio)propanoic acid	20.3	15.2	1.2	11.5	0.49
PETMeOx	2-(Ethylthio)acetic acid	16.3	13.3	1.2	29.4	0.42

[a] Carboxylic acid used for PEI acylation. [b] Determined by SEC in DMAc/LiCl. [c] Determined from the second heating DSC run.
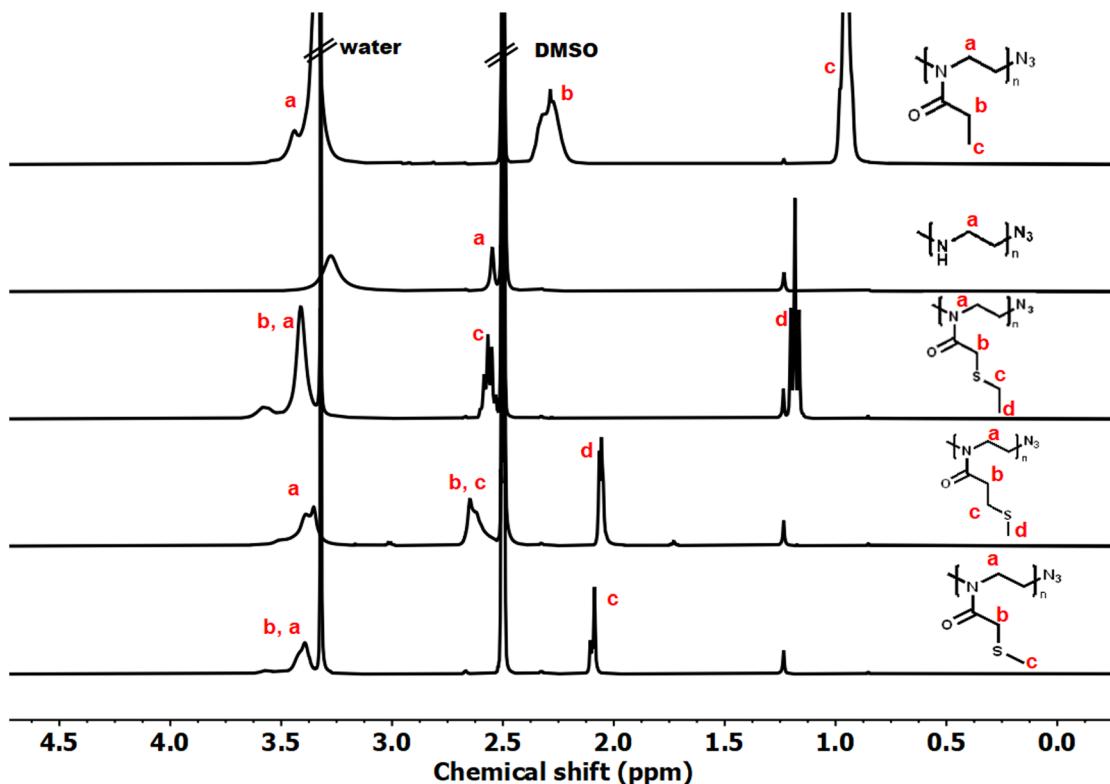
Fig. 1 Representative ^{1}H NMR spectra of PEtOx, PEI, PMTMeOx, PMTEtOx, and PETMeOx in DMSO-d_6.
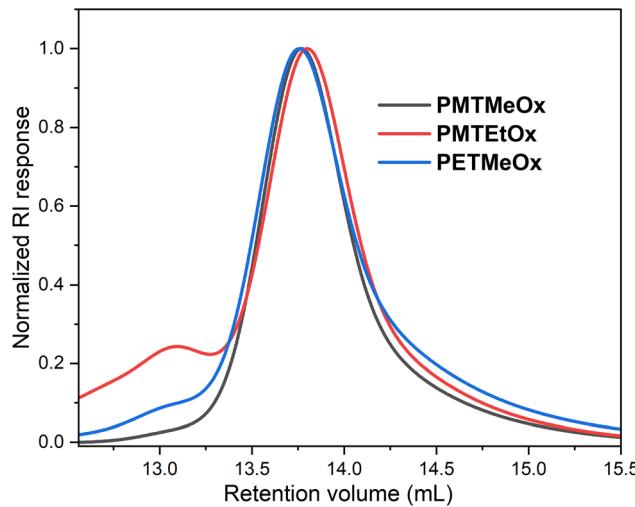
Fig. 2 SEC traces of the homopolymers eluted with DMAc/LiCl.
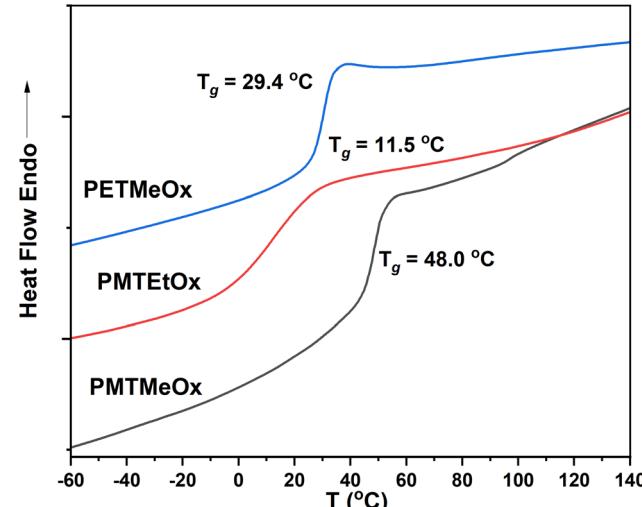
Fig. 3 DSC curves of the homopolymers.

accelerating chain association and dissociation, promoting a reproducible equilibrium in self-assembled structures, and (ii) the development of magnetic resonance imaging (MRI) contrast agents, enabling fast transverse relaxation and enhancing MRI contrast.[52] Additionally, these low-T_g polymers can serve as effective plasticizers, improving the mechanical properties of various polymer blends. All homopolymers synthesized in this study showed limited water solubility at room tempera-

ture. As such, they are highly promising candidates for stimuli-responsive systems, enabling rapid transitions from a hydrophobic to a hydrophilic state upon oxidation.

In a subsequent procedure, we used the PMTMeOx polymer as a hydrophobic block with oxidation-responsive properties to prepare amphiphilic diblock copolymers (Scheme 2). Nosylated PEG-macroinitiator (M_n = 2 kDa) was synthesized (Fig. S3 and S4†) and chain-extended with PEtOx of varying
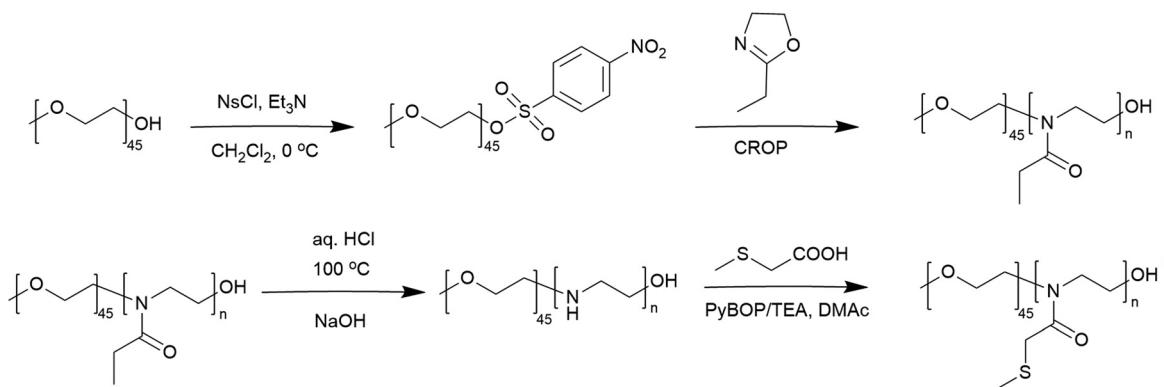
Scheme 2 Synthesis of thioether-containing PEG-*b*-PMTMeOx (*part of end groups might be acylated).

Table 2 Characteristics of PEG-*b*-PMTMeOx copolymers

Polymer	DP (target)	DP^a (measured)	$M_w{}^b$ (kDa)	$M_n{}^b$ (kDa)	$Đ^b$
PEG$_{45}$-*b*-PMTMeOx$_{30}$	30	26	11.7	10.1	1.1
PEG$_{45}$-*b*-PMTMeOx$_{60}$	60	46	17.4	15.5	1.1
PEG$_{45}$-*b*-PMTMeOx$_{100}$	100	109	25.2	22.8	1.2

^{a} DP of PMTMeOx block determined by ^{1}H NMR in CD$_3$OD. ^{b} Determined by SEC in DMAc/LiCl.

degrees of polymerization (DP = 30, 60, and 100) through CROP in acetonitrile (Table 2). To obtain PEG-*b*-PMTMeOx, the PEG-*b*-PEtOx copolymers were subjected to controlled acidic hydrolysis in aqueous hydrochloric acid, followed by reacylation methylthioacetic acid, using the hydrolysis/reacylation protocol mentioned above (Scheme 2).

These copolymers were characterized by ^{1}H NMR spectroscopy (Fig. 4). The spectra lacked imine signals from PEI at δ 2.77 ppm and showed new peaks assigned to PAOx side chains (δ 1.10 and 2.45 ppm). As with the homopolymers,

^{1}H/^{13}C HSQC NMR spectra were used for further structure confirmation to rule out potential signal overlaps (Fig. S5†). All polymers had well-defined structures with a low molar mass distribution ($Đ \sim 1.2$), as confirmed by size exclusion chromatography (SEC) analysis. Moreover, SEC analysis revealed a distinct shift in molecular weight from PEG to PEG-*b*-PEtOx and PEG-*b*-PMTMeOx as each subsequent block was added, accompanied by an increase in DP (Fig. 5).

Block copolymer nanoparticles were prepared using the solvent switch method.[53] The block copolymers were first dis-
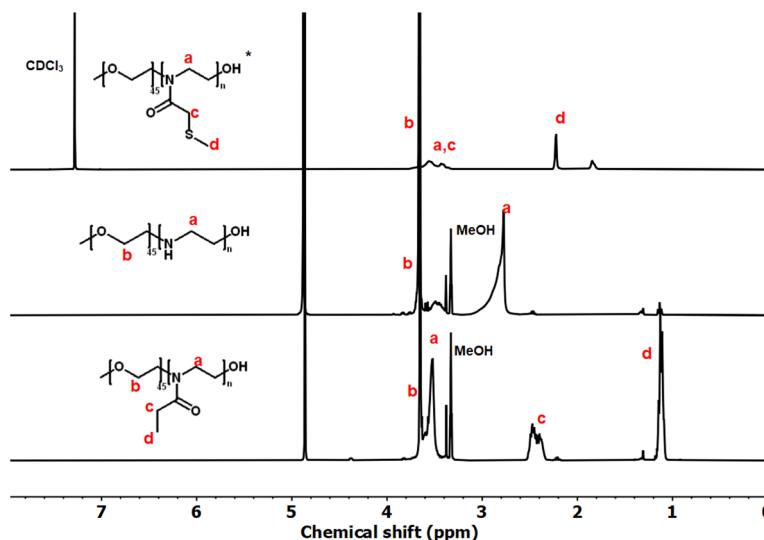
Fig. 4 ^{1}H NMR spectra of PEG-*b*-PMTMeOx in CDCl$_3$; and PEG-*b*-PEI and PEG-*b*-PEtOx, in CD$_3$OD (*some −OH groups were transformed into their respective esters).
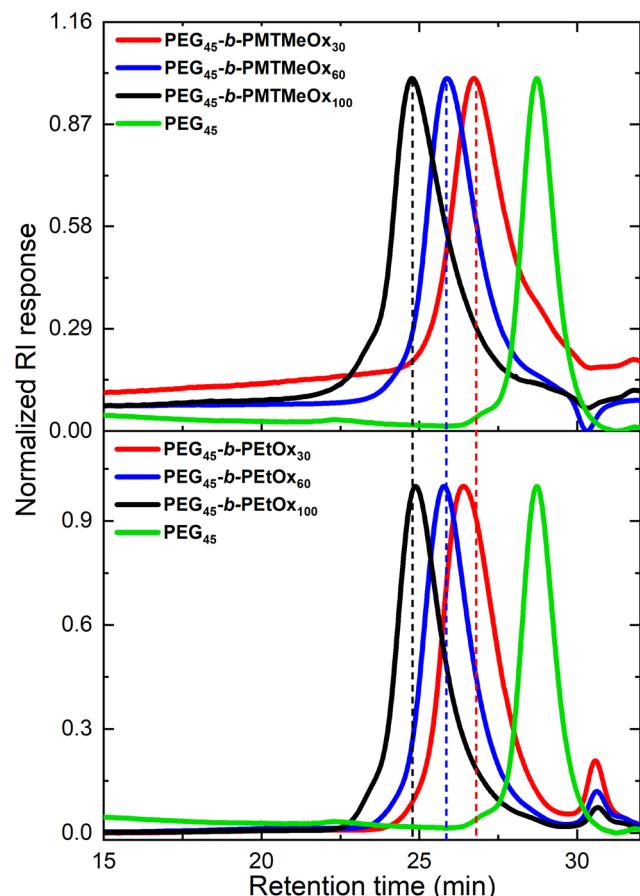
Fig. 5 SEC chromatograms of PEG, PEG-*b*-PEtOx, and PEG-*b*-PMTMeOx with different degrees of polymerizations.

solved in acetonitrile and then introduced to water to induce self-assembly, followed by evaporation of the organic solvent. The hydrodynamic sizes of the nanoparticles were assessed by DLS and TEM, revealing sizes ranging from 70 to 450 nm, which increased with the degree of polymerization (DP). TEM analysis of DP 30 nanoparticles indicated the presence of spherical micelles, together with aggregated clusters of approximately 60 nm, in line with our DLS measurement. Such clusters may result from hydrogen bonding interactions between the oxazoline and PEG chains (Fig. 6). However, gradual macroscopic aggregation was observed in DP 60 and 100 copolymer nanoparticles after several days of storage in an aqueous solution at room temperature. The aggregation of DP60 and DP100 copolymers might be attributed to the insufficient stabilization from the short PEG block (2 kDa). For this reason, we selected the DP 30 copolymer for further analysis of its oxidation-responsive disassembly.

PEG_{45}-$PMTMeOx_{30}$ nanoparticles disassembled in the presence of H_2O_2, as shown by DLS (Fig. 7). The light scattering intensity assessed in DLS measurements correlated with the particle size and/or concentration in the solution. The optimal scattering intensity should range from 100 to 500 kcps. Values exceeding this range indicate either inadequate dilution or high particle concentration. In contrast, values below this range suggest that the particles are too small or excessively diluted to be detected by the laser in DLS.

At the beginning of the experiment, the particle solutions showed a scattering intensity of 400–450 kcps, which fell within the acceptable range. However, incubation with 10 and 1 mM H_2O_2 exponentially decreased the light scattering intensity, which dropped below 100 kcps after 6 and 24 hours, respectively. After these intervals, only a minute fraction of particles was still detectable, thus demonstrating micelle disassembly. The dilution of polymer nanoparticles was very low (from 1 mg mL^{-1} to 0.83 mg mL^{-1}), which is still clearly above the critical micelle concentration of the polymer without added peroxide (DLS measurements showed the presence of micelles at 0.5 mg mL^{-1}).
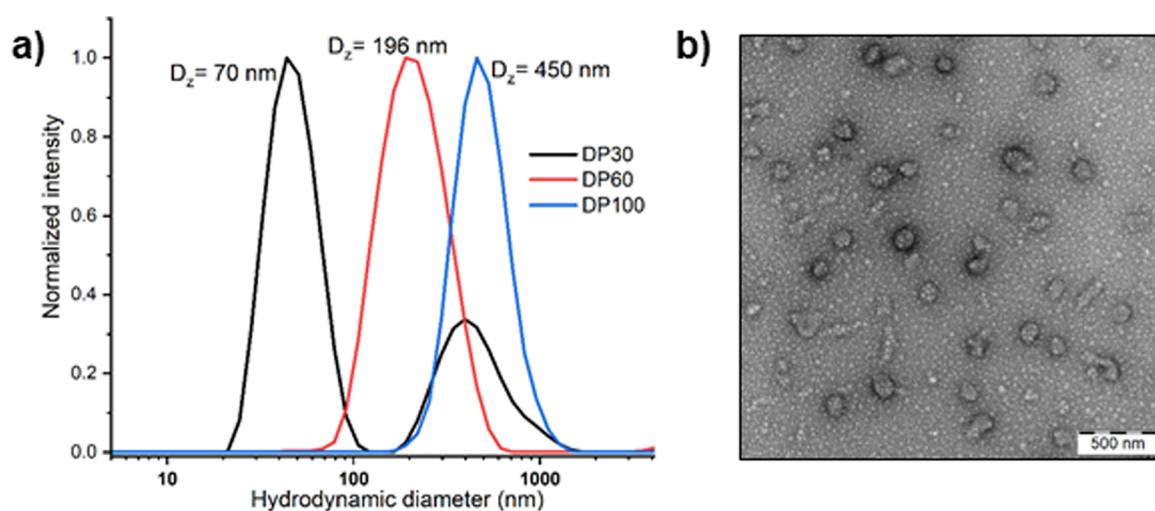
Fig. 6 (a) Hydrodynamic size distributions of PEG_{45}-$PMTMeOx_x$ micelles of different PMTMeOx DP measured by DLS in water (c_{pol} = 1 mg mL^{-1}) and (b) TEM image of PEG_{45}-*b*-$PMTMeOx_{30}$ nanoparticles.
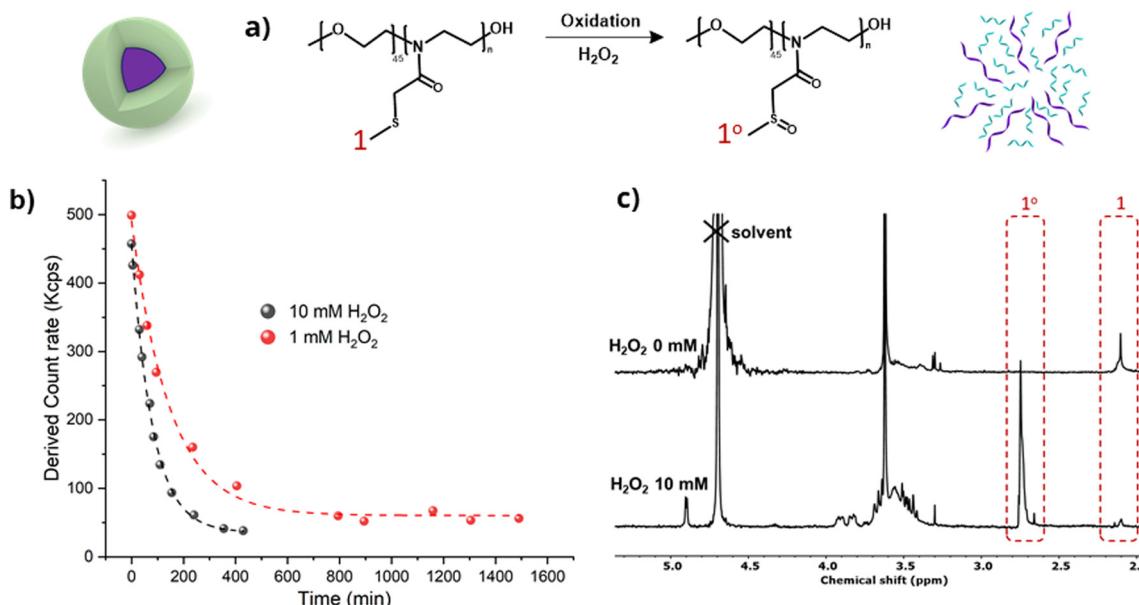
Fig. 7 (a) Schematic illustration of the oxidative reaction of PEG-*b*-PMTMeOx (DP = 30) block copolymer NPs with H_2O_2, (b) decrease of DLS scattering light intensity of the nanoparticle solution at 1 mg mL^{-1} when adding 1 and 10 mM H_2O_2 and (c) ^{1}H NMR spectra of PEG-*b*-PMTMeOx before and 24 hours after oxidation with 10 mM H_2O_2 in D_2O.

To gain insights into the molecular response to the polymer oxidation, the oxidation process was monitored by ^{1}H-NMR spectroscopy (Fig. 7c). The solution of oxidized nanoparticles treated with 10 mM H_2O_2 for 24 hours was subjected to gel filtration and lyophilization before analyzing the structures of the resulting solids by ^{1}H NMR (D_2O). The spectra clearly revealed noticeable shifts in the peaks corresponding to the methylene groups adjacent to the sulfide functionalities, confirming the oxidation of thioether to sulfoxide by H_2O_2. In addition, further partial oxidation of sulfoxides to sulfones cannot be entirely excluded, however, this is highly improbable due to the absence of NMR peaks at around 3 ppm.[54] Such oxidation disrupted the amphiphilic balance of the block copolymers, potentially leading to the dissociation of the spherical structures. These results are in line with the findings of our previous research on thioether-based polymer systems responsive to reactive oxygen species (ROS).[22,55]

ing the oxidation-responsiveness of these polymers, as confirmed by ^{1}H NMR analysis, revealing the conversion of thioether moieties to sulfoxides. Overall, the synthetic approach developed in this study provides a valuable strategy for the synthesis of oxidation-sensitive PAOx polymers, which hold great promise in the development of drug delivery systems and other biomedical applications. Further studies should explore the biocompatibility, drug encapsulation capabilities, and stimuli-responsiveness of these polymers to expand their utility in controlled drug release applications.

Author contributions

The manuscript was written through the contributions of all authors. All authors have approved the final version of the manuscript.

Conclusion

Oxidation-sensitive thioether-containing PAOx homopolymers can be easily prepared by reacylation of linear polyethyleneimine (PEI) with thioether-containing carboxylic acids. The resulting polymers show well-defined structures with low molar mass distributions, and low glass transition temperatures, making them suitable for various biomedical applications. Furthermore, these thioether-containing PAOx polymers can be used as hydrophobic blocks to prepare amphiphilic diblock copolymers with a polyethylene glycol (PEG) shell and a thioether-containing PAOx core. Treatment with hydrogen peroxide destabilizes the micellar structures, demonstrat-

Conflicts of interest

The authors have no conflicts to declare.

Acknowledgements

References

1 D. Daubian, J. Gaitzsch and W. Meier, *Polym. Chem.*, 2020, **11**, 1237–1248.

2 C. G. Palivan, R. Goers, A. Najer, X. Zhang, A. Car and W. Meier, *Chem. Soc. Rev.*, 2016, **45**, 377–411.

3 Y. Mai and A. Eisenberg, *Chem. Soc. Rev.*, 2012, **41**, 5969.

4 A. Rösler, G. W. M. Vandermeulen and H.-A. Klok, *Adv. Drug Delivery Rev.*, 2001, **53**, 95–108.

5 D. Babuka, K. Kolouchova, L. Loukotova, O. Sedlacek, O. Groborz, A. Skarkova, A. Zhigunov, E. Pavlova, R. Hoogenboom, M. Hruby and P. Stepanek, *Macromolecules*, 2021, **54**, 10667–10681.

6 K. Kataoka, A. Harada and Y. Nagasaki, *Adv. Drug Delivery Rev.*, 2001, **47**, 113–131.

7 G. Wang, P. Huang, L. Wang, X. Chen, Y. Zhou, W. Huang and D. Yan, *SmartMat*, 2022, **3**, 522–531.

8 A. Puglisi, E. Bayir, S. Timur and Y. Yagci, *Biomacromolecules*, 2019, **20**, 4001–4007.

9 S. Bener, A. Puglisi and Y. Yagci, *Macromol. Chem. Phys.*, 2020, **221**, 2000109.

10 L. Xu, H. Wang, Z. Chu, L. Cai, H. Shi, C. Zhu, D. Pan, J. Pan, X. Fei and Y. Lei, *ACS Appl. Polym. Mater.*, 2020, **2**, 741–750.

11 Y. Kotsuchibashi, *Polym. J.*, 2020, **52**, 681–689.

12 P. Švec, O. V. Petrov, J. Lang, P. Štěpnička, O. Groborz, D. Dunlop, J. Blahut, K. Kolouchová, L. Loukotová, O. Sedláček, T. Heizer, Z. Tošner, M. Šlouf, H. Beneš, R. Hoogenboom and M. Hrubý, *Macromolecules*, 2022, **55**, 658–671.

13 M. Manzano and M. Vallet-Regí, *Chem. Commun.*, 2019, **55**, 2731–2740.

14 M. E. Roth-Konforti, M. Comune, M. Halperin-Sternfeld, I. Grigoriants, D. Shabat and L. Adler-Abramovich, *Macromol. Rapid Commun.*, 2018, **39**, 1800588.

15 A. Zhang, K. Jung, A. Li, J. Liu and C. Boyer, *Prog. Polym. Sci.*, 2019, **99**, 101164.

16 E. Jäger, V. Sincari, L. J. C. Albuquerque, A. Jäger, J. Humajova, J. Kucka, J. Pankrac, P. Paral, T. Heizer, O. Janouskova, R. Konefał, E. Pavlova, O. Sedlacek, F. C. Giacomelli, P. Pouckova, L. Sefc, P. Stepanek and M. Hruby, *Biomacromolecules*, 2020, **21**, 1437–1449.

17 M. Criado-Gonzalez and D. Mecerreyes, *J. Mater. Chem. B*, 2022, **10**, 7206–7221.

18 I. Piergentili, P. R. Bouwmans, L. Reinalda, R. W. Lewis, B. Klemm, H. Liu, R. M. De Kruijff, A. G. Denkova and R. Eelkema, *Polym. Chem.*, 2022, **13**, 2383–2390.

19 Q. Xu, C. He, C. Xiao and X. Chen, *Macromol. Biosci.*, 2016, **16**, 635–646.

20 Z. Zhou, Y. Wang and P. Hu, *Int. J. Nanomed.*, 2022, **17**, 2447–2457.

21 L. Yu, M. Zhang, F.-S. Du and Z.-C. Li, *Polym. Chem.*, 2018, **9**, 3762–3773.

22 F. H. Sobotta, M. T. Kuchenbrod, F. V. Gruschwitz, G. Festag, P. Bellstedt, S. Hoeppener and J. C. Brendel, *Angew. Chem., Int. Ed.*, 2021, **60**, 24716–24723.

23 J. M. Harris, M. D. Bentley, R. W. Moreadith, T. X. Viegas, Z. Fang, K. Yoon, R. Weimer, B. Dizman and L. Nordstierna, *Eur. Polym. J.*, 2019, **120**, 109241.

24 T. Lorson, M. M. Lübtow, E. Wegener, M. S. Haider, S. Borova, D. Nahm, R. Jordan, M. Sokolski-Papkov, A. V. Kabanov and R. Luxenhofer, *Biomaterials*, 2018, **178**, 204–280.

25 Z. M. Sahin, T. B. Kohlan, A. E. Atespare, M. Yildiz, S. Unal and B. Dizman, *J. Appl. Polym. Sci.*, 2022, **139**, e52406.

26 O. Sedlacek, B. D. Monnery, S. K. Filippov, R. Hoogenboom and M. Hruby, *Macromol. Rapid Commun.*, 2012, **33**, 1648–1662.

27 O. Sedlacek and R. Hoogenboom, *Adv. Thermoelectr.*, 2020, **3**, 1900168.

28 G. Gil Alvaradejo, M. Glassner, R. Hoogenboom and G. Delaittre, *RSC Adv.*, 2018, **8**, 9471–9479.

29 G. Vancoillie, W. L. A. Brooks, M. A. Mees, B. S. Sumerlin and R. Hoogenboom, *Polym. Chem.*, 2016, **7**, 6725–6734.

30 S. Bener, G. Yilmaz and Y. Yagci, *ChemPhotoChem*, 2021, **5**, 1089–1093.

31 H. Phan, R. Cavanagh, D. Destouches, F. Vacherot, B. Brissault, V. Taresco, J. Penelle and B. Couturaud, *ACS Appl. Polym. Mater.*, 2022, **4**, 7778–7789.

32 A. S. Gubarev, B. D. Monnery, A. A. Lezov, O. Sedlacek, N. V. Tsvetkov, R. Hoogenboom and S. K. Filippov, *Polym. Chem.*, 2018, **9**, 2232–2237.

33 L. Simon, V. Lapinte, L. Lionnard, N. Marcotte, M. Morille, A. Aouacheria, K. Kissa, J. M. Devoisselle and S. Bégu, *Int. J. Pharm.*, 2020, **579**, 119126.

34 M. A. Cortez and S. M. Grayson, *Macromolecules*, 2010, **43**, 4081–4090.

35 S. Jana and R. Hoogenboom, *Polym. Int.*, 2022, **71**, 935–949.

36 A. Krieg, C. Weber, R. Hoogenboom, C. R. Becer and U. S. Schubert, *ACS Macro Lett.*, 2012, **1**, 776–779.

37 K. Kempe, M. Lobert, R. Hoogenboom and U. S. Schubert, *J. Polym. Sci., Part A: Polym. Chem.*, 2009, **47**, 3829–3838.

38 O. Sedlacek, B. D. Monnery and R. Hoogenboom, *Polym. Chem.*, 2019, **10**, 1286–1290.

39 R. Hoogenboom, H. M. L. Thijs, M. W. M. Fijten, B. M. Van Lankvelt and U. S. Schubert, *J. Polym. Sci., Part A: Polym. Chem.*, 2007, **45**, 416–422.

40 C. Legros, M.-C. De Pauw-Gillet, K. C. Tam, S. Lecommandoux and D. Taton, *Eur. Polym. J.*, 2015, **62**, 322–330.

41 A. C. Rinkenauer, L. Tauhardt, F. Wendler, K. Kempe, M. Gottschaldt, A. Traeger and U. S. Schubert, *Macromol. Biosci.*, 2015, **15**, 414–425.

42 K. Kempe, *Macromol. Chem. Phys.*, 2017, **218**, 1700021.

43 O. Sedlacek, O. Janouskova, B. Verbraeken and R. Hoogenboom, *Biomacromolecules*, 2019, **20**, 222–230.

44 O. Sedlacek, D. Bera and R. Hoogenboom, *Polym. Chem.*, 2019, **10**, 4683–4689.

45 W.-L. Wang, K. Kawai, H. Sigemitsu and R.-H. Jin, *J. Colloid Interface Sci.*, 2022, **627**, 28–39.

46 T. Kagiya, S. Narisawa, T. Maeda and K. Fukui, *J. Polym. Sci., Part B: Polym. Lett.*, 1966, **4**, 441–445.

47 D. A. Tomalia and D. P. Sheetz, *J. Polym. Sci., Part A-1: Polym. Chem.*, 1966, **4**, 2253–2265.

48 T. G. Bassiri, A. Levy and M. Litt, *J. Polym. Sci., Part B: Polym. Lett.*, 1967, **5**, 871–879.

49 W. Seeliger, E. Aufderhaar, W. Diepers, R. Feinauer, R. Nehring, W. Thier and H. Hellmann, *Angew. Chem., Int. Ed. Engl.*, 1966, **5**, 875–888.

50 N. E. Göppert, M. Kleinsteuber, C. Weber and U. S. Schubert, *Macromolecules*, 2020, **53**, 10837–10846.

51 H. M. L. Lambermont-Thijs, F. S. Van Der Woerdt, A. Baumgaertel, L. Bonami, F. E. Du Prez, U. S. Schubert and R. Hoogenboom, *Macromolecules*, 2010, **43**, 927–933.

52 J. Wahsner, E. M. Gale, A. Rodríguez-Rodríguez and P. Caravan, *Chem. Rev.*, 2019, **119**, 957–1057.

53 C. Fetsch, J. Gaitzsch, L. Messager, G. Battaglia and R. Luxenhofer, *Sci. Rep.*, 2016, **6**, 33491.

54 A. J. Van Der Vlies, J. Xu, M. Ghasemi, C. Bator, A. Bell, B. Rosoff-Verbit, B. Liu, E. D. Gomez and U. Hasegawa, *Biomacromolecules*, 2022, **23**, 77–88.

55 G. Wang, P. Huang, M. Qi, C. Li, W. Fan, Y. Zhou, R. Zhang, W. Huang and D. Yan, *ACS Omega*, 2019, **4**, 17600–17606.